Session 02d (Poster): Precambrian sediments as records of early earth tectonics and ocean-atmosphere-biosphere interactions
Poster # 24

Banded Iron Formations from the Eastern Desert of Egypt: A new type of Ore?

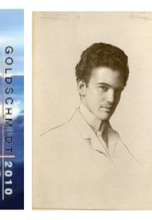

KHALIL, Khalil Isaac[1] **and EL-SHAZLY, Aley K.**[2]

[1] Department of Geology, University of Alexandria, Egypt
[2] Geology Department, Marshall University, Huntington, WV 25755

Abstract

Banded iron formations (BIFs) occur in thirteen localities in an area approximately 30,000 km^2 within the eastern desert of Egypt. With the exception of the southernmost deposit of Um Nar which is suspected to be pre-Panafrican, all other BIFs are considered Neoproterozoic in age. The iron ore occurs as rhythmically layered bands, groups of bands or separate lenses that reach a maximum thickness of 100 m, and which are intercalated with volcanic arc assemblages dominated by andesitic lava flows, tuffs and lapilli tuffs, and basaltic pyroclastics. In most cases, the BIFs contain syn-sedimentary structures such as bedding and lamination. The entire sequence of BIFs and host rocks is strongly deformed and regionally metamorphosed under greenschist to amphibolite facies conditions.

All thirteen deposits are comprised of an oxide facies consisting of magnetite and hematite, and a silicate facies consisting of quartz with subordinate amounts of one or more of the minerals: chlorite (ripidolite - clinochlore), greenalite, stilpnomelane, garnet (grossular – almandine), carbonate (mainly calcite), epidote, hornblende, or plagioclase. With the exception of the northernmost jaspilite type deposit of Hadrabia, magnetite is the predominant oxide, where it seems to be primary, even when martitized. Major and trace element compositions of the Egyptian BIFs show significant variations from one deposit to another. The most intriguing geochemical feature of the investigated BIFs is their high Fe/Si ratio in comparison with Algoma and Superior types. Based on Fe/Si ratios, these deposits are classified into two groups; a) fresh BIFs with Fe/Si ratio < 2.3 (e.g. Um Nar, Gebel El Hadid and Wadi El Dabbah) and b) altered BIFs with Fe/Si ratio > 3.0 (e.g. Gebel Semna, Hadrabia and Abu Merwat).

The relatively small nature of individual deposits, strong variations in Fe_2O_3(t) and SiO_2 contents and the enrichment in Cr, V and Ni (for a few deposits) support a volcanic exhalative source for Fe and Si, leading most scientists to classify them as "Algoma type BIFs". On the other hand, the lack of sulfides, varve – like nature of some deposits, and lack of a distinct enrichment in Co, Ni, Cu, As, and Sr are at odds with such a classification. Finally, the Neoproterozoic age of Egyptian BIFs, high Fe and P contents, and presence of diamictites intercalated with at least one of these deposits compels a comparison with the Rapitan type deposits.

The presence of laminations and absence of wave generated structures in most Egyptian BIFs indicate subaqueous precipitation below wave base. The formation of authegenic primary magnetite as the most abundant mineral instead of hematite reflects precipitation away from the shore and under slightly euxinic conditions in basins where S and CO_2 activities were low. The paucity of primary sulfides and pure siderite in the Egyptian BIFs support this interpretation and may also indicate formation away from the deepest parts of the basin. Accordingly, we suggest that the Egyptian BIFs formed in the deepest "shelf – like" environments of fore-arc and back-arc basins. These characteristics may indeed justify the definition of a new type of BIF.

Geologic Setting

The banded iron ore deposits occur intercalated with volcanosedimentary units within the basement of the Egyptian Eastern Desert. These units, amalgamated during the Neoproterozoic Pan-African Orogeny, reveal a history that can be simplified into five distinct tectonic stages (Fig. 1; Table 1; e.g. El-Gaby et al., 1990; Stern et al., 2006): (i) rifting and breakup of Rodinia 900 – 850 Ma; (ii) sea floor spreading (870 – 750 Ma); (iii) subduction and development of arc – back-arc basins (750 – 650 Ma); coupled with episodes of intrusion of the "older" granitoids; (iii) accretion/ collision marking the culmination of the Pan-African Orogeny; (iv) continued shortening coupled with escape tectonics and continental collapse; and (v) intrusion of the alkalic, post-orogenic "Younger Granites".

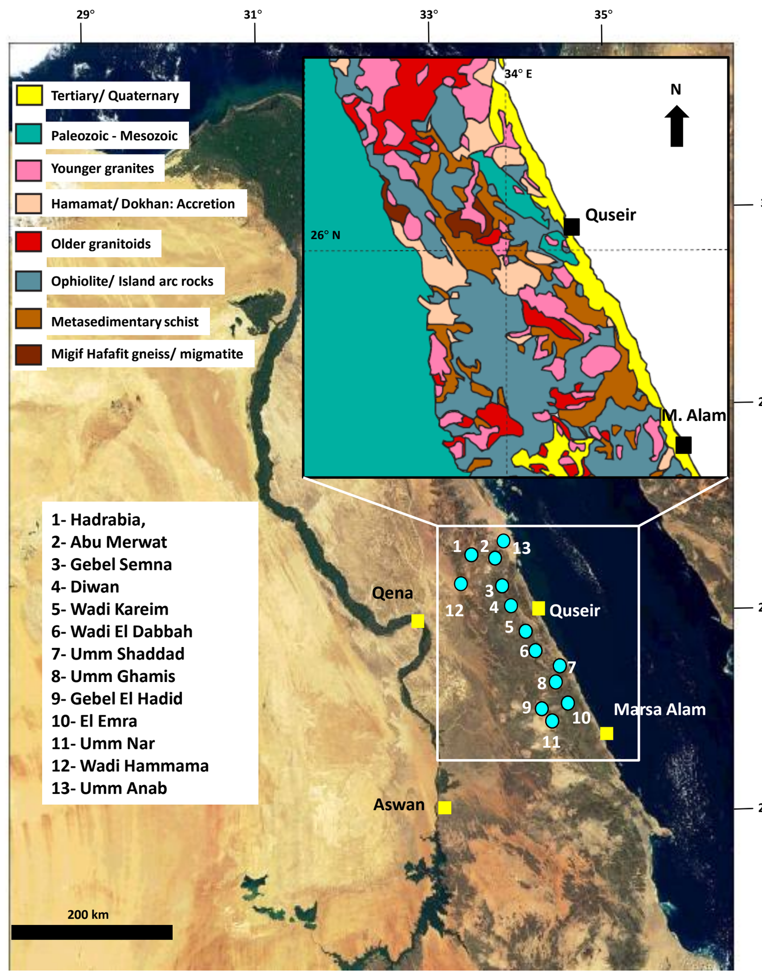

Fig. 1: Thematic Landsat image of Egypt showing the location of eleven of the most important banded iron-ores (blue circles). Inset is a simplified geological map of the area outlined in the white rectangle (from Egyptian Geological Survey, 1981). Key is given in Table 1 and explained in the "Geologic Setting" section.

Table 1: Tectonostratigraphic basement units of the Egyptian Eastern Desert

Eon/ Era	Tectonic Stage		Age Ma	Rock Types/ Associations		Granitoid intrusion
Phanerozoic	Post-Orogenic		< 570	Younger Granites (post-tectonic, alkalic): Granite, granodiorite, monzonite.		Gattarian (570 – 475 Ma)
Neoproterozoic	PanAfrican	Accretion/ Collision	650 - 570	Dokhan metavolcanics (andesite, rhyolite, rhyodacite, pyroclastics) intercalated with Hammamat metasediments (breccias, conglomerates, greywackes, arenites, and siltstones)		
		Subduction	750 - 650	Island Arc	Shadhli Metavolcanics (rhyolite, dacite, tuff); Volcaniclastic metasediments; Diamictites (Strutian: 680 – 715 Ma). Banded Iron Ores	Meatiq (710 – 610) Hafafit (760 – 710)
		Spreading	850 - 750	Ophiolite	Tholeiitic basalt, sheeted dykes, gabbros, serpentinites, all weakly metamorphosed	Shaitian Granite (850 – 800 Ma)
Archean?/ Paleoproterozoic	Pre-Pan-African		<1.8 Ga	Metasedimentary schists and gneisses (Hb-, Bt-, and Chl- schists), metagreywackes, slates, phyllites, and metaconglomerates Some BIF? Umm Nar?		
				Migiff – Hafafit gneiss (Hb and Bt gneiss) and migmatite		

Sources: Egyptian Geological Survey (1981); El-Gaby et al. (1990); Hassan and El-Hashad (1990); Stern et al. (2006); Avigad et al. (2007); Moussa et al. (2008).

Table 2: BIF from the Eastern Desert of Egypt compared to the main types of BIF

	Algoma	Superior	Rapitan	Egyptian BIF "Fresh"	Egyptian BIF "Altered"
Age (Ga)	> 2.5	2.5 – 1.9	0.8 – 0.6	0.85? – 0.65	0.75-0.6
Size	small	large	small	small	small
Thickness	< 50 m	> 100 m	75 – 270 m	v. thin	5 – 30 m
Deformation	V. strong	Undeformed	Deformed	Strong	Strong
Facies	O,Si,Sf±C	O,Si,C	O,Si,±C	O,Si,±C	O,Si,±C
Oolites	rare	always	common	none	none
Ore Minerals	Mgt>Hm	Mgt>Hm higher Hm	Hm	Mgt>Hm	Mgt≥Hm
Rock Associations	Thol to CA vol., tuffs, wackes/ shales	Carbonaceous shales	Diamictites	CA volcanic, tuffs, shales wackes; diamictites?	
Chemistry	High Cr, Mn, Ni, Cu, As	Low Cr, Co, Ni, Cu, Zn.	High P,Fe, low Cr, Co, Ni	Low Cr, Co, Ni, Cu variable Al	
REE/NASC	+ Eu, - Ce, slight HREE-enrichment	+ Eu, Strong HREE-enrichment	Weak + Eu v. strong HREE enrichment	-Sm, Ce? +Nd & Eu, HREE – rich?	+Eu, -Yb LREE-rich
Fe/Si	< 1.36	< 1.36	1.3 – 1.6	1.4 – 2.75	3 – 4.7
Fe_2O_3/FeO	1.9	2.76	46 - 100	5.5 - 8	7 - 57

O = oxide, Si = silicate, C = carbonate, Sf = sulfide, Mgt = magnetite, Hm = hematite.

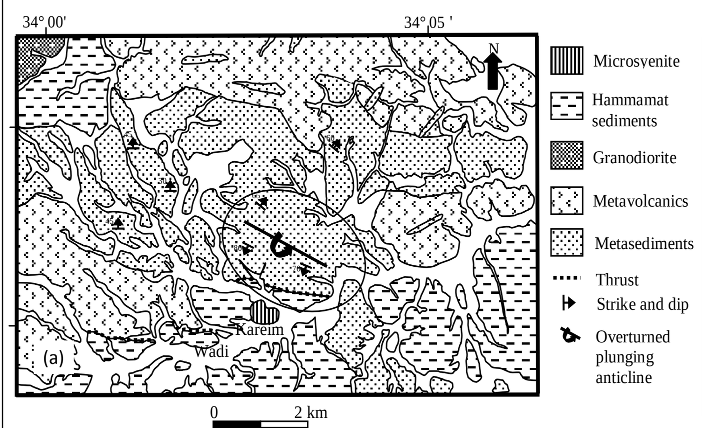

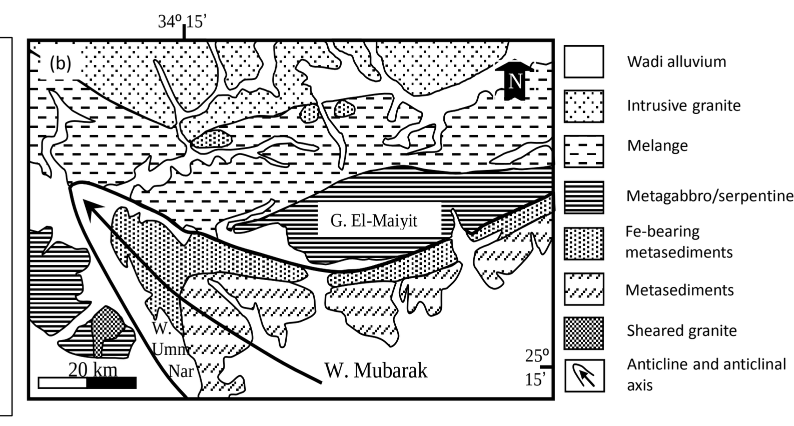

Fig. 2: Geological maps of (a) Wadi Kareim area (modified from El-Habaak and Mahmoud, 1994 and Noweir et al. 2004) and (b) Umm Nar (after El-Aref et al., 1993). Ellipse in (a) shows location of banded iron ore.

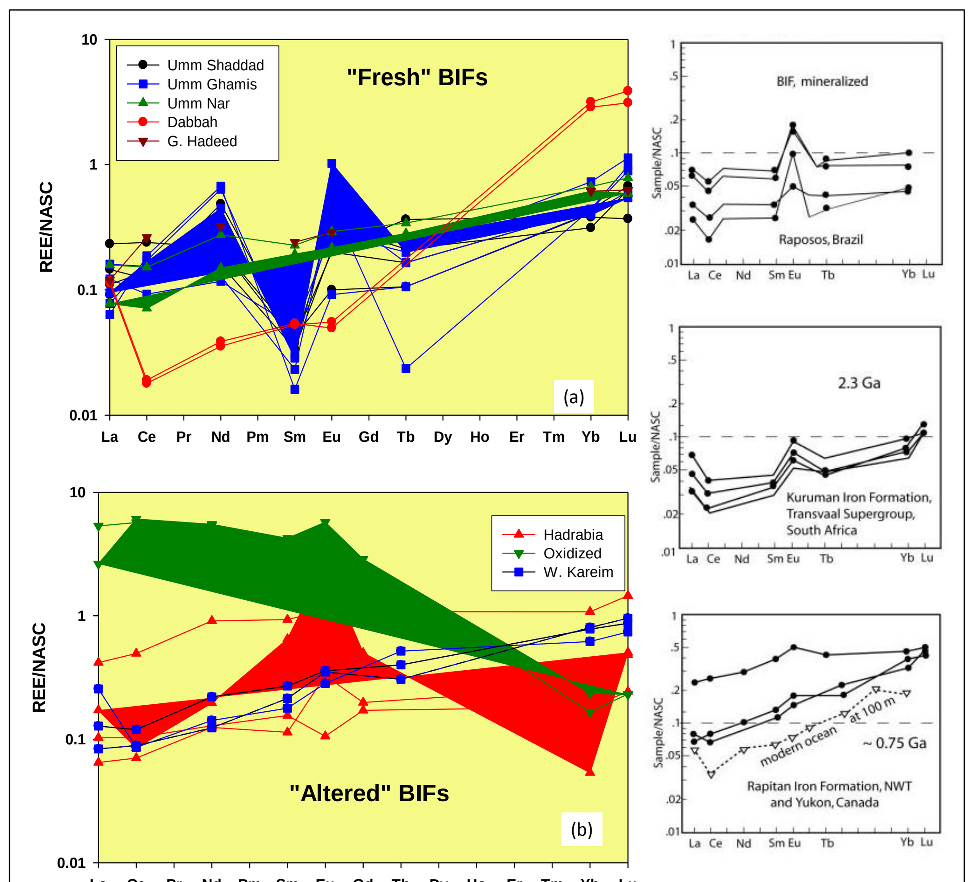

Fig. 9: REE patterns normalized relative to North American Shale Composite (NASC) for (a) "fresh" BIF from Takla et al. (1999); El-Habaak & Soliman, (1999); (b) "altered" BIF from Hadrabia (Essawy et al.,1997), and Kareim (El-Habaak and Soliman (1999) compared to patterns typical of Algoma (c), Superior (d), and Rapitan (e). (c) – (e) from Klein (2005).

Characteristics of the Egyptian banded iron ores

- ❖ Occur as sharply defined stratigraphic units within a sequence of Neoproterozoic island-arc tholeiitic to andesitic/dacitic lava flows interlayered with pyroclastics (Figs. 1 & 2). Only one deposit is suspected to be Paleoproterozoic in age (Umm Nar; El-Aref et al., 1993).
- ❖ Some deposits (e.g. Wadi Kareim) are reportedly associated with diamictites (e.g. Stern et al., 2006) suggesting some relation to glaciations and possibly "Snowball Earth" conditions.
- ❖ The lateral extents and thicknesses of individual ore bodies are relatively small, typically on the order of tens of meters (Fig. 2).
- ❖ The entire sequence (iron ore + host rocks) is strongly deformed by a series of folds and thrusts, and was regionally metamorphosed under at least greenschist facies conditions.
- ❖ Deformation evident on the regional, outcrop, and hand specimen scales (Figs. 2 , 3a & b).
- ❖ Rhythmic banding is either streaky (Umm Ghamis) or continuous (Hadrabia) where layers of magnetite and hematite alternate with quartz – rich layers on macro-, meso- or micro-scales (Figs. 3c - e).
- ❖ Hadrabia is the only deposit with oolitic and pisolitic textures. None of the other deposits have oolites, pisolites, pellets, or granules (Essawy et al., 1997). Other wave generated primary structures are also lacking.
- ❖ Oxide and silicate facies ubiquitous; carbonate facies usually represented by calcite is common in several deposits (e.g. Wadi Kareim, Wadi Dabbah, and Hadrabia). Sulfide facies is generally lacking.
- ❖ Magnetite is dominant, except in a few deposits (e.g. Hadrabia) where hematite ≃ magnetite. Most crystals of magnetite have undergone some grain coarsening attributed to metamorphism in several areas (e.g. Wadi Kareim; Fig. 4a).
- ❖ Magnetite commonly altered to martite, specularite, or goethite (Figs. 4b – e) due to post-metamorphic oxidation.
- ❖ Silicate facies characterized by the minerals: chlorite, epidote, garnet, hornblende, and stilpnomelane (Figs. 4g, h, & i).
- ❖ Some deposits are also strongly altered, often developing a porous texture (Fig. 3f).
- ❖ Many of the iron ore deposits (e.g. Gebel Semna, Gebel Hadrabia and Abu Merwat) are characterized by high Fe and low Si contents in comparison with Algoma, Superior, or Rapitan BIF types (Fig. 7, Table 2), whereas others (e.g. Gebel El Hadid and Wadi El Dabbah) are characterized by Fe/Si ratios somewhat comparable to Rapitan BIF. Altered samples with a porous texture are typically characterized by some of the highest Fe/Si ratios (Khalil, 2001; 2006; 2008).

Are the Egyptian Banded Iron Ores Unique?

The size and general characteristics of the Egyptian BIF led to the suggestion that they are "Algoma type" deposits (e.g. Sims and James, 1984; Table 2). However, several points suggest that the Egyptian BIFs may be unique, namely:

- ❖ Algoma and Superior type deposits are Late Archean or Paleoproterozoic in age (e.g. Klein, 2005), whereas the Egyptian BIF's are Neoproterozoic (Fig. 5). Only Umm Nar is *suspected* to be Paleoproterozoic (El-Aref et al., 1993).
- ❖ The Neoproterozoic Rapitan/ Urucum type deposits are typically jaspilites associated with glacial deposits. Among the Egyptian iron ores, only Hadrabia is characterized by Hm ≥ Mgt? (Essawy et al., 1997). Diamictites have only been reported from Wadi Kareim (Stern et al., 2006).
- ❖ Egyptian BIFs are intercalated with calcalkalic metavolcanic and metapyroclastic rocks of island arc affinity rather than the tholeiites typical of Algoma type deposits.
- ❖ Sulfide facies is lacking, carbonates minor, usually predominated by calcite (or ankerite) rather than siderite; well developed silicate facies with stilpnomelane, chlorite, epidote, and garnet; oxide facies predominated by magnetite.
- ❖ Garnet in many Egyptian BIFs is grossular rich (and in some cases free of almandine; Khalil, 2001; Takla et al., 1999) unlike garnets from Algoma or Superior BIFs which are typically almandine – spessartine solid solutions (e.g. Klein and Beukes, 1993).
- ❖ Amphibole in many Egyptian BIFs is a magnesiohornblende (e.g. Takla et al., 1999; Khalil, 2001) rather than cummingtonite – grunerite.
- ❖ Chlorite in all Egyptian BIFs is a clinochlore – ripidolite with significantly higher Mg/(Fe + Mg) ratios (0.5 – 0.7) compared to Algoma and Superior type BIFs (Fig. 6).
- ❖ All Egyptian BIFs characterized by an unusually high Fe/Si ratio (Fig. 7), as well as higher Fe^{3+}/Fe^{2+} ratios compared to Algoma and Superior types (Fig. 8). Fe/Si is considerably higher for BIFs affected by alteration (hydrothermal or weathering?).
- ❖ Egyptian BIFs characterized by bulk chemistries that vary considerably from one deposit to another. However, many deposits are characterized by high Al and low Cr and Ni compared to Algoma type BIFs (Table 2).
- ❖ REE patterns for Egyptian BIFs vary from one deposit to another, and do not resemble those patterns characteristic of Algoma, Superior, or Rapitan BIFs. "Fresh" Umm Ghamis and Umm Shaddad have prominent negative Sm and positive Nd and Eu anomalies, and slight HREE enrichment (Fig. 9a). Hadrabia deposit ("altered") is characterized by a positive Eu anomaly. Strongly oxidized samples from Hadrabia show LREE enrichment relative to North American Shale Composite (NASC) (Fig. 9b).

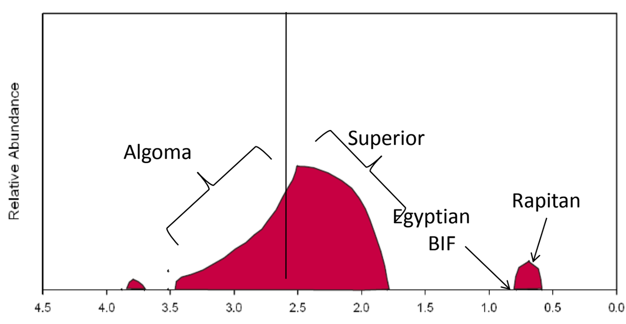

Fig. 5: Schematic diagram showing age and abundance of the three main types of BIF relative to Hamersley Group as a maximum (from Klein, 2005). Note Egyptian BIF age.

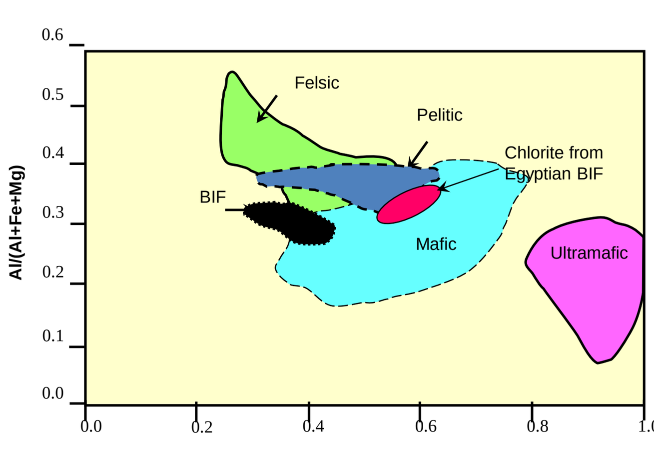

Fig. 6: Compositional range for chlorites from the silicate facies of the Egyptian BIF relative to the fields of Sheikhikhou (1992).

Conclusions

Egyptian BIFs share many of the characteristics of each of the main types of BIF. Features that make these deposits unique include their Neoproterozoic ages, association with calcalkalic rather than tholeiitic volcanics, magnetite as the main ore mineral, lack of wave generated textures and structures, unusually high Fe/Si ratios, high Al, and low Cr, Ni and Co compared to Algoma BIF, and variable REE patterns that lack a Ce anomaly, but may show a negative Sm and positive Eu and Nd anomalies.

Although not all Egyptian BIFs had identical histories, they share many genetic aspects. They all formed in several small back- arc basins in which volcanism associated with active spreading increased the concentration of Fe^{2+} in sea water. Primary magnetite was precipitated below wave base, possibly during a period of glacial ice melting. The deposits were deformed and metamorphosed during the culmination of the Panafrican Orogeny. Hydrothermal alteration ± weathering later affected some of these deposits resulting in the leaching of SiO_2, and concentration of Fe in the "altered" deposits. This stage may have also led to the oxidation of the ore.

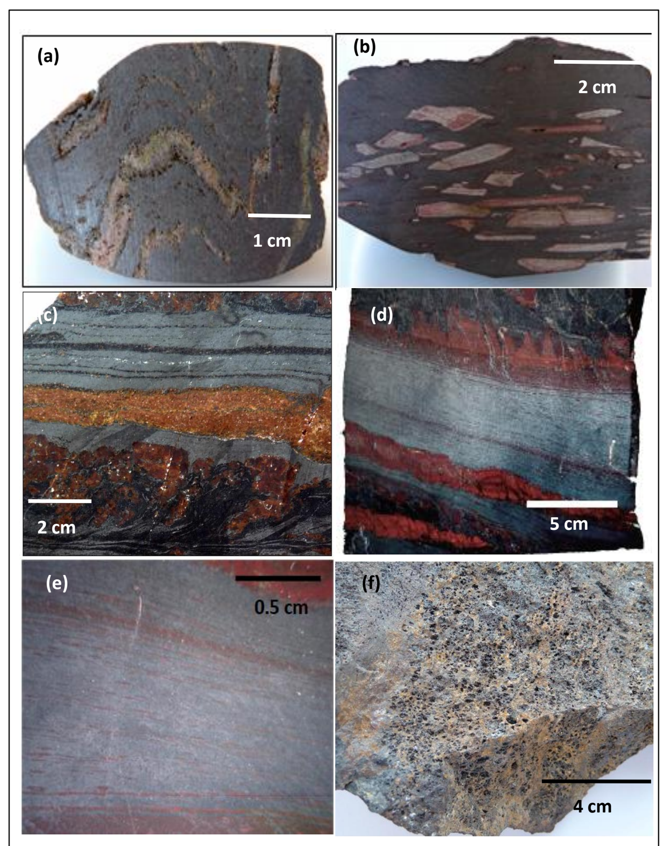

Fig. 3: Strong folding (a) and brecciation of chert (b) in oxide facies samples from Umm Nar. (c) Macro- and meso- scale banding in least altered BIF sample from Gebel Semna. (d) Meso- and (e) micro-scale banding (lamination) between alternating jasper (red) and Fe-ore in unaltered samples from Wadi Kareim. (f) Altered sample with a highly porous texture from Gebel Semna.

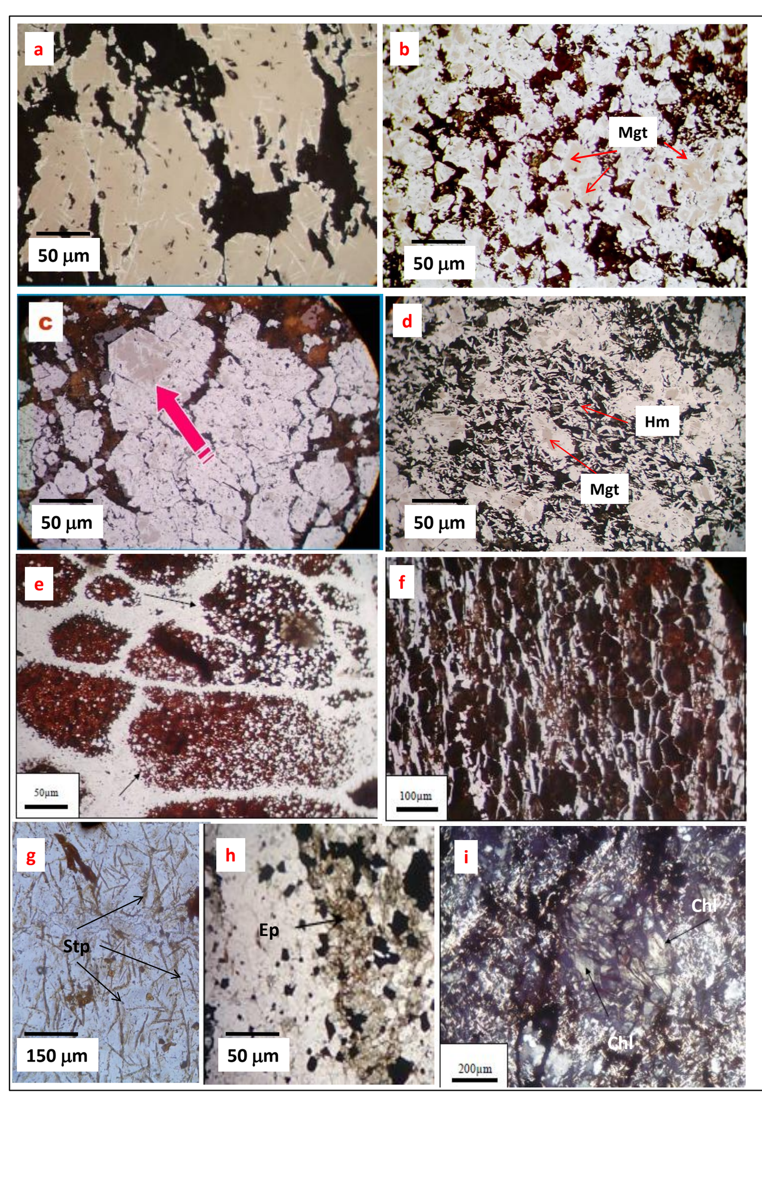

Fig. 4: Photomicrographs showing selected textural relations. (a) through (e) taken under polarized reflected light, oil immersion; (f) - (h) under plane polarized transmitted light. (a) Magnetite coarsened by metamorphism, Wadi Kareim; (b) relicts of primary? magnetite (Mgt) replaced by hematite, Wadi Kareim; (c) coarse grained porphyroblasts of strongly martitized magnetite, Wadi Kareim; (d) relict magnetite strongly martitized, and transformed into platy specular hematite (Hm) Wadi Kareim; (e) primary magnetite (arrow) and quartz embedded in a matrix of secondary goethite, Gebel Semna; (f) oriented platy hematite, oxide facies, strongly altered porous sample from Gebel Semna; (g) fibrous stilpnomelane (Stp) in silicate facies; Wadi Kareim; (h) epidote (Ep; arrow) coexisting with magnetite, silicate facies; Wadi Kareim; (i) chlorite coexisting with sericite and quartz, silicate facies; Gebel Semna; cross polarized transmitted light.

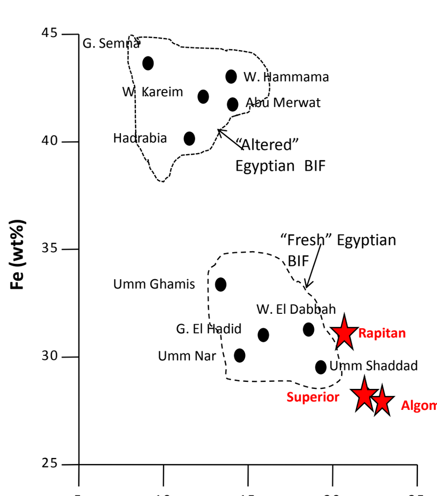

Fig. 7: Bulk rock compositions of "Fresh" and "Altered" BIFs from Egypt relative to Algoma, Superior, and Rapitan average compositions from Gross & McLeon (1980).

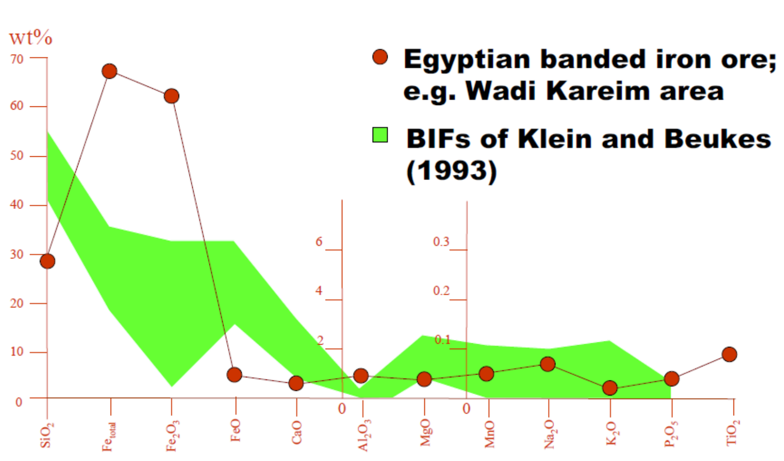

Fig. 8: Bulk rock major oxide components of Wadi Kareim iron formation (solid circles) compared to overall averages for Algoma and Superior type BIFs (shaded green) from Klein (2005). All analyses recalculated on an anhydrous, CO_2 – free basis.

References

Avigad, D., Stern, R., Beyth, M., Miller, N., and McWilliams, M. O., 2007. Precambrian Research, 154: 88 – 106.
Egyptian Geological Survey, 1981. Geological Map ofEgypt. Available from http://library.wur.nl/isric/kaart/origineel/afr_egg.jpg
El- Aref, M.M., El Doudgdoug, A., Abdel Wahed, M. and El Manawi, A.W., 1993. Mineral. Deposita, 28, 264-278.
El -Gaby, S., List, F.K., and Tehrani, R., 1990. *in*: Said, R., ed., The Geology of Egypt, Balkema, Rotterdam, 175–184.
El-Habaak, G.H., Mahmoud, S., 1994. Egypt. Journal of African Earth Science, 19, 125-133.
El-Habaak, G.H., & Soliman, M.F., 1999. Fourth International Conference on Geochemistry, Alexandria University, Egypt., 149-169.
Essawy, M.A., Zalata, A.A., Makroum, F., 1997. Egyptian Mineralogist, 9, 147-168.
Gross, G.A., and McLeon, C.R., 1980. The Canadian Mineralogist, 18, 223-229.
Hassan, M.A. and Hashad, A.H., 1990. *in* Said, R., ed., the geology of Egypt, Balkema, Rotterdam, 201-245.
Khalil, K.I., 2001. Fifth International Conference on Geochemistry, Alexandria University, 333-352.
Khalil K.I., 2006. 7th International Conference On Geochemistry, Alexandria University, Egypt, Sep. 6-7 (Abstract).
Khalil K.I., 2008. 8th International Conference On Geochemistry, Alexandria University, Egypt. (Abstract).
Klein, C. 2005. American Mineralogist, 90: 1473 – 1499.
Klein, C., and Beukes, N.J., 1993. In: Condie, K.C., (ed.). Development in Precambrian Geology: Proterozoic crustal evolution. 10, 383-418.
Moussa, M., Stern, R., Manton, W. I., and Ali, K., 2008. Precambrian Research, 160: 341 – 356.
Noweir, M.A., Ghoneim, M.F., Abu Alam, T.S., 2004. Sixth International Conference on Geochemistry, Alexandria University. Egypt, I-B, 821-847.
Sims, P.K., James, H.L., 1984. Economic Geology 79, 1777-1784.
Stern, R. J., Avigad, D., Miller, N.R., and Beyth, M., 2006. Journal of Afrcian Earth Sciences, 44: 1-20.